

First Principles Investigation of Ferromagnetism for $Zn_{1-x}Mn_xY$ ($Y = S, Se, Te$)

N. Benkhattou* and D. Bensaid

Department of Physics, Faculty of sciences, University of Sidi Bel Abbes, Algeria

Abstract: Through first-principles full-potential linear muffin-tin orbital (FP-LMTO) method within the local density approximation, we investigate the structural and electronic properties of $Zn_{1-x}Mn_xY$ ($Y = S, Se, Te$) where Y represent an element of the VIa column (S, Se and Te) compounds-based diluted magnetic semiconductors (DMS) in the Zinc-blend structure. We have investigated the lattice parameters and band gap energies. The lattice constants *a* are found to change linearly for the $Zn_{1-x}Mn_xTe$ and $Zn_{1-x}Mn_xS$ alloy.

Pacs Number (s): 61.66.Dk; 71.22.+I; 71.20.Nr

Keywords: FP-LMTO, DFT, band structures calculations, DMS, bowing gap.

INTRODUCTION

Recently, diluted magnetic semiconductors (DMS) have attracted the attention of the academic and industrial communities, since they can be used in developing spintronics, integrated optoelectronic devices, and nano-structured quantum devices, because spin-related phenomena as well as carrier transport can be manipulated in a well-controlled semiconductor system [1-4]. II-VI compounds show in addition novel magneto-optical and magneto-transport properties if the cation is partly substituted by Mn with its half-filled 3d shell. The interaction between Mn 3d electron and the electronic states of the host crystal is of special interest [5].

The variation in the relative intensities of the Mn 3d features by changing the anion in a compounds series, like $Cd_{1-x}Mn_xY$ or $Zn_{1-x}Mn_xY$ ($Y = S, Se, Te$), is promising to clarify the amount of p-d hybridization in these alloys.

In this paper, we investigate the magnetism of ZnS, ZnSe and ZnTe based DMSs based on ab initio electronic structure calculations in order to have clues about the origin of the ferromagnetism in DMSs [6-8]. In a II-VI compound, transition metal (TM) impurities do not introduce any carriers, therefore, we can discuss effects of carrier doping separately from a concentration of TM impurities. In addition to that, detailed investigation on the feasibility of II-VI compound-based DMS is of great importance from the industrial view point, because it is easy to dope TM impurities into II-VI compounds up to several ten percent [9].

Calculation

The electronic structure calculations of the DMS are performed based on the local density approximation with the parameterization by Perdew-Wang [10]. For the (FP-LMTO) calculations, we have used the available computer code Lmto [11].

We employ the muffin-tin approximation to describe the crystal potential, and the wave functions in each Muffin-tin

sphere are expanded with real spherical harmonics up to $l_{max} = 6$. The k integration over Brillouin zone is performed using the tetrahedron method [12].

ZnS, ZnSe, and ZnTe have the zinc blende crystal structure, and their lattice constants are $a = 5.4093 \text{ \AA}$, $a = 5.6676 \text{ \AA}$ and $a = 6.089 \text{ \AA}$, respectively. Muffin-tin radii are chosen so that they touch with each other

RESULTS AND DISCUSSION

Structural Properties

We first calculated the structural properties of the binary compounds ZnSe, ZnTe, ZnS and MnTe, MnSe, MnS in the zincblende structure. As for the semiconductor ternary alloy in the type $B_{1-x}A_xC$, we have started our FP-LMTO calculation of the structural properties with the zinc-blende structure and let the calculation forces to move the atoms to their equilibrium positions. For divers concentrations $x = 0.25, 0.5, 0.75$. We perform the structural optimization by calculating the total energies for different volumes around the equilibrium cell volume V_0 of the binary and their alloy. The calculated total energies are fitted to the Murnaghan's equation of state [13] to determine the ground state properties such as the equilibrium lattice constant a_0 , the bulk modulus B and its pressure derivative B' . The calculated equilibrium parameters (a_0, B and B') are given in Table 1 Our results are compared with the experiment and with the FP-LAPW (method) results.

Usually, in the treatment of alloys, it is assumed that the atoms are located at the ideal lattice sites and the lattice constant varies linearly with the composition x according to the so-called Vegard's law [14]:

$$a_{(A_xB_{1-x}C)} = xa_{AC} + (1-x)a_{BC}, \quad (1)$$

where a_{AC} and a_{BC} are the equilibrium lattice constants of the binary compounds AC and BC, respectively, and $a_{(A_xB_{1-x}C)}$ is the alloy lattice constant. The obtained equilibrium lattice constant, of the ferromagnetic $Zn_{1-x}Mn_xY$ ($Y = S, Se, Te$) semi-magnetic semiconductors are given in Table 1.

The equilibrium lattice parameter of the zinc-blende $Zn_{1-x}Mn_xTe$ and $Zn_{1-x}Mn_xS$. We found a good agreement with

*Address correspondence to this author at the Department of Physics, Faculty of sciences, University of Sidi Bel Abbes, Algeria; Tel/Fax: (213) 48 54 43 44; E-mail: nordine_bt@yahoo.com

Table 1. The Calculated Lattice Parameter *a*, the Bulk Modulus *B* and its Pressure Derivative *B'* for $Zn_{1-x}Mn_xY$ ($Y = S, Se, Te$) and its Binary Compounds

$Zn_{1-x}Mn_xTe$				$Zn_{1-x}Mn_xSe$				$Zn_{1-x}Mn_xS$			
x	a	B	B'	x	a	B	B'	x	a	B	B'
0	6.05	51.11	4.68	0	5.607	66.74	3.85	0	5.334	82.28	4.41
Exp	6.089 ^a	50.9 ^a	5.04 ^a	Exp	5.667 ^k	64.7 ^k	4.77 ^k	Exp	5.409	5.432	
Theo	6.027 ^b	55.67 ^b	4.9 ^b	Theo	5.578 ^l	71.84 ^l	4.599 ^l	Theo	5.027 ^m		
0.25	5.95	60.82	4.08	0.25	5.53	76.96	3.67	0.25	5.244	95.46	4.29
Exp	6.0428 ^c	-	-	Exp				Exp			
Theo	6.043 ^d	54.18 ^d	4.11 ^d	Theo				Theo			
0.5	5.85	66	5.85	0.5	5.41	93.98	16.51	0.5	5.134	104.34	6.32
Exp	6.225 ^e	-	-	Exp				Exp			
Theo	6.215 ^f	-	-	Theo				Theo			
0.75	5.76	89.24	4.13	0.75	5.33	112.33	4.84	0.75	5.027	141.044	3.73
Exp	6.286 ^g	-	-	Exp				Exp			
Theo	-	-	-	Theo				Theo			
1	5.65	91.47	5.62	1	5.28	130.83	5.01	1	4.937	184.26	2.41
Exp	6.337 ^h	37 ⁱ	-	Exp				Exp			
Theo	6.303 ^j	50 ⁱ	-	Theo				Theo			

^a Ref [15], ^b Ref [16], ^c Ref [17], ^d Ref [18], ^{e, i, j} Ref [19], ^{f, g} Ref [20], ^h Ref [21], ^k Ref [22], ^l Ref [23], ^m Ref [24].

the experiment on the other. We have determined the equilibrium lattice parameter of the zinc-blende MnY ($Y = S, Se, Te$), which is found to be underestimated compared to the experimental.

The equilibrium lattice constants *a* shows a linear variation versus Mn concentration of $Zn_{1-x}Mn_xS$ and $Zn_{1-x}Mn_xTe$, but a small deviation from Vegard's law is clearly visible for the $Zn_{1-x}Mn_xSe$.

There are no results to compare with our values. Thus finds new values for various concentrations, our result to take as reference. Fig. (1), show the variation of the calculated equilibrium lattice constant versus concentration *x* for $Zn_{1-x}Mn_xY$ ($Y = S, Se, Te$). The Mn mole fraction (*x*) was determined by using the linear relation: $a(x) = -0.4044X + 5.3374$ (\AA°).

Obtained for lattice parameter of $Zn_{1-x}Mn_xS$ and lattice parameter for $Zn_{1-x}Mn_xSe$ vary according to the linear relation: $a(x) = -0.3416X + 5.6022$ (\AA°).

Fig. (2) shows the variation of the bulk modulus versus concentration. The bulk modulus grew linearly with the composition Mn for the $Zn_{1-x}Mn_xSe$.

We observe in Fig. (2) that bulk modulus grew with concentration (*x*) and with the nuclear charge of the element of the VIa column.

Electronic Properties

The calculated band structure energies of binary compounds as well as their alloy using FP-LMTO method within LDA approximation exhibit a direct band gap at Γ point for $Zn_{1-x}Mn_xY$ ($Y = Zn, Se, S$) with *x* vary between 0.25 and

0.75, the valence band maximum (VBM) and the conduction

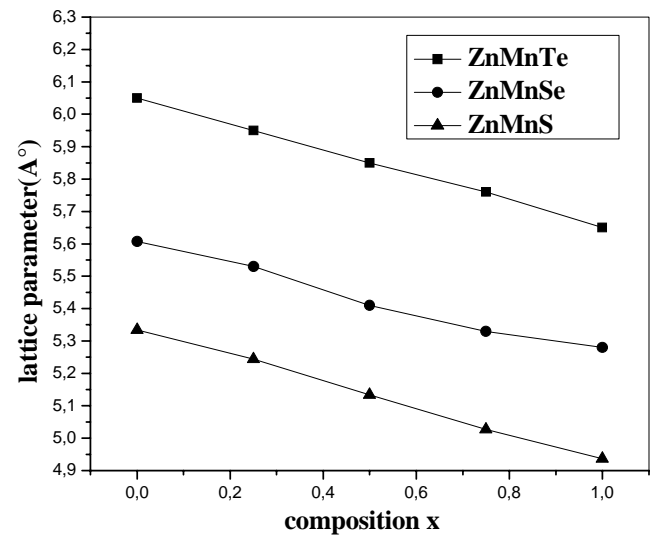


Fig. (1). Variation of the calculated equilibrium lattice constant versus concentration *x* for $Zn_{1-x}Mn_xY$ ($Y = S, Se, Te$).

band minimum (CBM) occur at the Γ and X, respectively. The important features of the band structure (main band gaps) are given in Table 2.

As well as the theoretical and experimental ones. It is clearly seen that the band gap are underestimated in comparison with experiment results. This underestimation of the band gaps is mainly due to the fact that the simple form of LDA does not take into account the quasiparticle self-energy correctly [25].

The carrier induced ferromagnetism by hole doping was observed in (Zn, Mn) Te [32], and II–VI based-DMSs have been of much interest also from the scientific point of view. Taking these aspects into account, it is important to investigate the carrier induced effects in ZnS, ZnSe and ZnTe based DMSs.

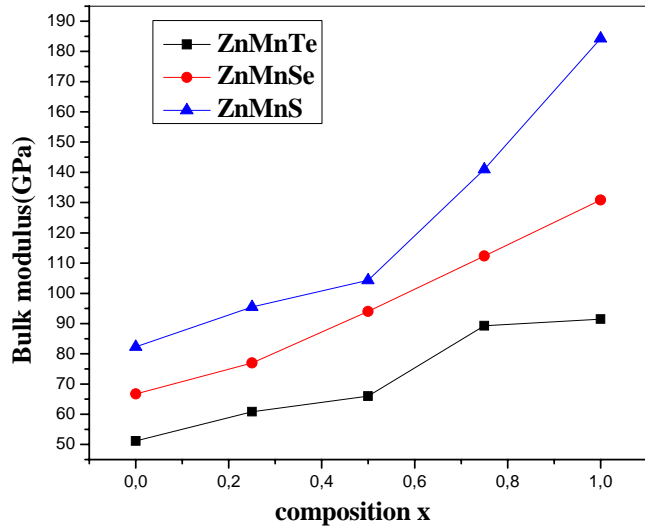


Fig. (2). Variation of the calculated bulk modulus versus concentration x for $Zn_{1-x}Mn_xY$ ($Y = S, Se, Te$).

Table 2. Direct ($\Gamma-\Gamma$) and Indirect ($\Gamma-X$) Band Gaps of BeSe and ZnSe and Their Alloy at Equilibrium Volume

$Zn_{1-x}Mn_xSe$			
$\Gamma-\Gamma(\Gamma-X)$			
x	Present	Exp	Others
0	1.2(3.5)	2.82 ^a (4.3 ^c)	2.76 ^b 2.5 ^d
(4.54 ^b)			
0.25	1.38		
0.5	0.27(0.24)		
0.75	0.29(0.283)		
1	3.65(3.2)	2.9 ^e	
$Zn_{1-x}Mn_xS$			
0	2.16(4.55)	2.71 ^e	2.11(GGA) ^f
0.25	1.186(0.52)		
0.5	0.3		
0.75	0.285(0.288)		
1	4.5(3.8)	3.4 ^e	
$Zn_{1-x}Mn_xTe$			
0	1.041 (2.2)	2.38 ^g	2.19(2.25) ^g
0.25	1.33	2.42 ^h	2.37 ⁱ
0.5	0.14	2.55 ^j	2.49 ^k
0.75	0.28	2.74 ^l	-
1	2.14	3.2 ^m	2.7 ⁿ

^a Ref [33], ^b Ref [34], ^c Ref [35], ^d Ref [36], ^e Ref [17], ^f Ref [37], ^g Ref [38], ^h Ref [39], ⁱ Ref [40], ^j Ref [41], ^k Ref [42], ^l Ref [43], ^m Ref [44], ⁿ Ref [45].

Electron Band Structures and Densities of States

In order to elucidate underlying mechanism of the ferromagnetism in II–VI compound-based DMSs, the density of states (DOS) is calculated. Figs. (3-5) shows the DOS of 25% TM-doped ZnTe based DMSs in the ferromagnetic state. It is found that the impurity states appear in the band gap.

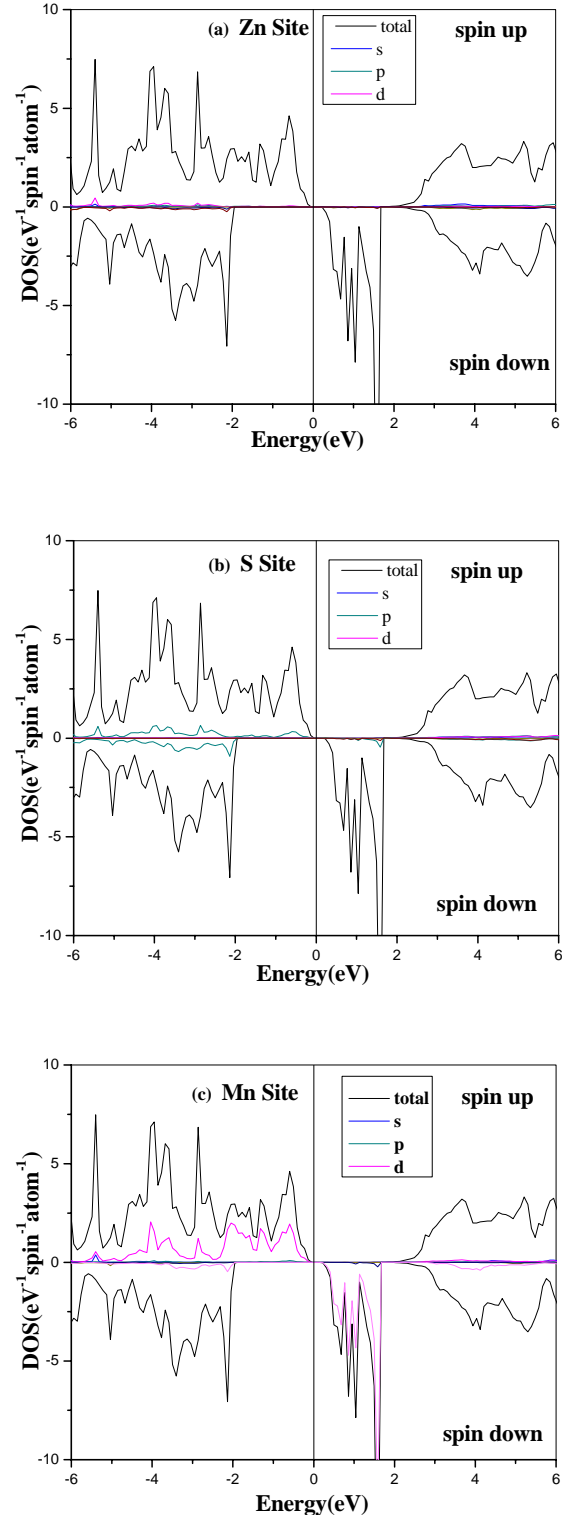


Fig. (3). DOS for the ferromagnetic $Zn_{1-x}Mn_xS$ for spin up and spin down.

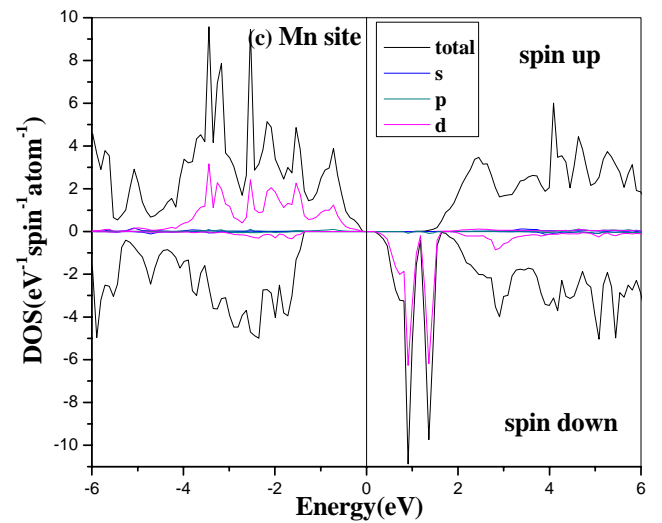
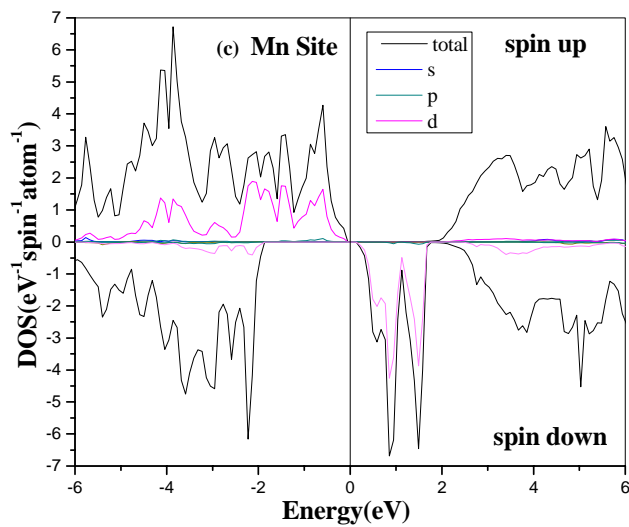
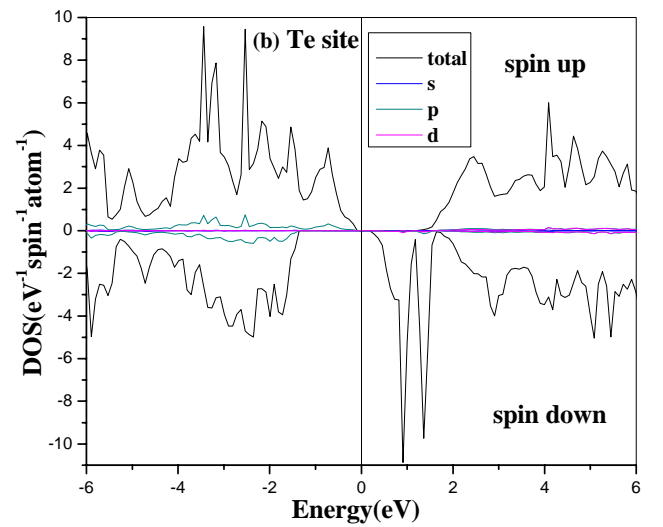
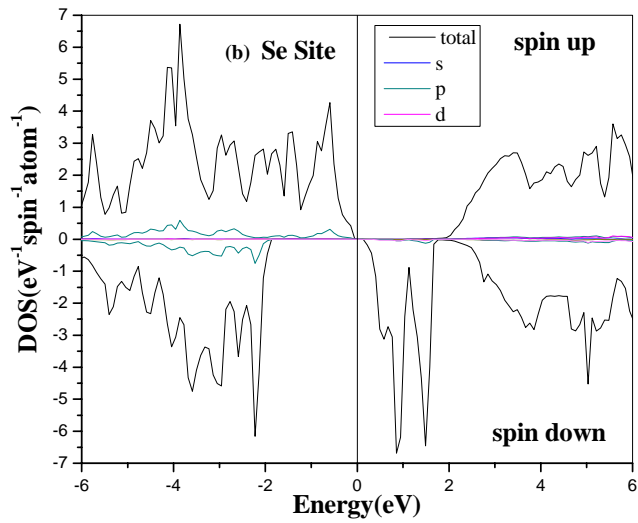
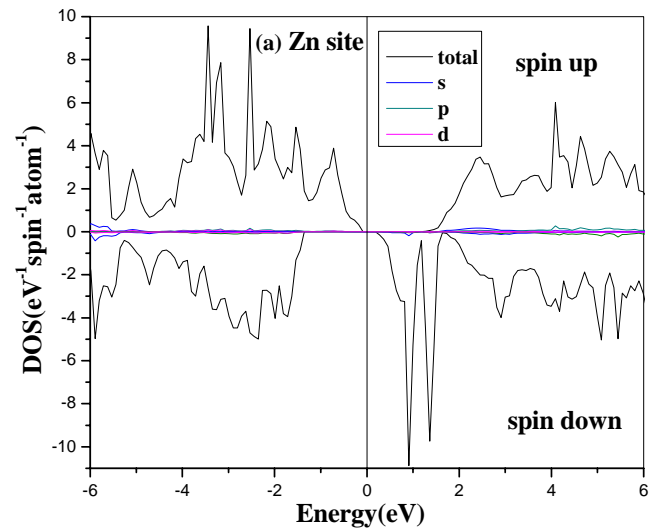
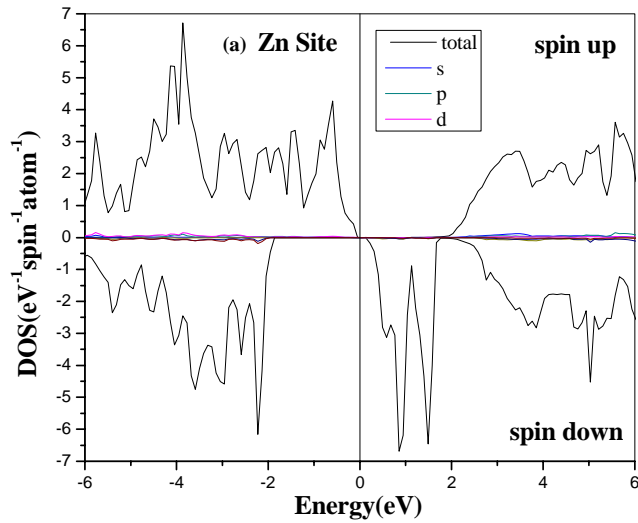


Fig. (4). DOS for the ferromagnetic $\text{Zn}_{1-x}\text{Mn}_x\text{Se}$ for spin up and spin down.

Fig. (5). DOS for the ferromagnetic $\text{Zn}_{1-x}\text{Mn}_x\text{Te}$ for spin up and spin down.

The spin-polarized band structures of ferromagnetic ZnMnTe, ZnMnS and ZnMnSe compounds at the calculated lattice constants are depicted in Figs. (3-5).

The figures show for each compound, the band structures corresponding to spin up and down alignments. We have referenced the zero energy at the top of the valence band for spin up. The bottom of the conduction bands and the top of the valence bands are at the Γ point in the Brillouin zone, it is well known that the calculations of the local densities of states (DOS) serve as a qualitative description of the atomic and orbital origins of the various band states. We illustrate our calculations of DOS in Figs. (3-5) for ZnMnS and ZnMnSe, ZnMnTe, respectively. The spin-dependent density of states (DOS) for the ferromagnetic phase is presented in Fig. (2, upper panel). The lower panel presents the contributions to the DOS from the Mn-3d orbitals. We can see that the upper valence band complex has Mn d and Te p characteristics, which differ widely for spin up and spin down. On the other hand, there strong contribution of the Mn spin down states to the valence band. We observe also that the spin up Mn d band is occupied (Figs. 3c, 4c, 5c), and centered at $E_V^\uparrow = -3.42eV$ for ZnMnTe and at $E_V^\uparrow = -4.15eV$ for ZnMnSe, and at $E_V^\uparrow = -4.06eV$ for ZnMnS whereas the spin down d band is empty (Figs. 3c, 4c) and 5(c)), and centered at $E_V^\downarrow = +1.37eV$ for ZnMnTe and at $E_V^\downarrow = +1.5eV$ for ZnMnSe, and at $E_V^\downarrow = +1.57eV$ for ZnMnS where E^\uparrow and E^\downarrow denote the valence band maxima (VBM) for spin up and spin down, respectively. The negative values obtained, for ZnMnTe and for ZnMnSe, and for ZnMnS indicate that the effective potential for the minority spin is more attractive than that for the majority spin, as is usually the case in spin-polarized systems [26]. It has been shown that ferromagnetic band structure calculations can be used to estimate the exchange constants $N_0\alpha$ and $N_0\beta$. Assuming the usual K onto interactions, $N_0\alpha$ and $N_0\beta$ are defined as [27]. Where ΔE_c and ΔE_v are the band edge spin splitting of the valence bands and conduction bands, respectively, and $\langle S \rangle$ is the average Mn spin. We have calculated the exchange constant by evaluating the spin splitting of the conduction and valence bands, which mimics a typical magneto-optical experiment [28].

We summarize in Table 2 our results of ΔE_c , ΔE_v , $N_0\alpha$ and $N_0\beta$ for both ZnMnY ($Y = S, Se, Te$).

Magnetic Properties

Our calculated total and local magnetic moments as well as that of the interstitial site are given in Table 3. It is expected in Mn doped DMSs [29] that: (i) the number of valence minority spin electrons is not changed by the Mn impurity and (ii) each Mn impurity adds five additional majority spin states to the valence band. In Table 3 we show that this description is also valid for ZnMnTe and ZnMnSe and ZnMnS.

The total magnetic moment of materials ZnMnY ($Y = S, Se, Te$) equal $\approx 5\mu_B$ (μ_B is the Bohr magneton).

From Table 3 we can see that the p-d hybridization is found to reduce the local magnetic moment of Mn.

We observed the small local magnetic moments on the nonmagnetic S, Se, Te and Zn sites.

Table 3. Calculated Magnetic Moments (in Bohr Magneton μ_B of Several Sites and the Total Magnetic Moment for Each Mn for the Ferromagnetic ZnMnY ($Y = S, Se, Te$) with 25%

Site	ZnMnTe	ZnMnSe	ZnMnS
Mn	4.053	3.826	3.8225
Zn	0.0334	0.0422	0.0384
Te	0.0459	-	-
Se	-	0.0699	-
S	-	-	0.0888
Interstitial site	0.671	0.775	0.694
Total μ_B	5.0029	4.99	4.756

Site	ZnMnTe	ZnMnSe	ZnMnS
ΔE_c	0.13 [0.19 ^a]	0.57	0.485
ΔE_v	-1.05 [1.14 ^a]	-1.69	-1.55
$N_0\alpha$ This work	0.208	0.912	0.776
exp	0.18 ^b	0.26 ^c	-
Theo	0.304 ^a	-	-
$N_0\beta$ This work	-1.68	-2.704	-2.48
exp	-1.05 ^b	-1.31 [$x \leq 10.3$] ^c	-
Theo	-1.83 ^a	-	-

^a Ref [17], ^b Ref [30], ^c Ref [31].

CONCLUSION

We have presented in this paper the structural and electronic properties and magnetic moments of the ZnMnY ($Y = S, Se, Te$), with 25% Mn in the ferromagnetic phase. For FP-LMTO method within the LSDA approximation for exchange-correlation potential.

We have calculated the composition dependence of the lattice constant, bulk modulus, the bulk modulus for alloy increase with the Mn concentration.

We have also determined the exchange constants $N_0\alpha$ and $N_0\beta$. The calculations of total and local magnetic moments have shown that every Mn impurity adds no hole carriers to the perfect ZnY ($Y = S, Se, Te$) crystal, and that the total magnetic moment is equal to $5\mu_B$.

REFERENCES

- [1] Ohno H. Making nonmagnetic semiconductors ferromagnetic. Science 1998; 281: 951-86.
- [2] Ohno Y, Young DK, Beschoten B, Matsukura F, Ohno H, Awschalom DD. Electrical spin injection in a ferromagnetic semiconductor heterostructure. Nature 1999; 402: 790-2.
- [3] Ohno H, Munekata H, Penney T, von Molnar S, Chang LL. Magnetotransport properties of p-type (In, Mn)As diluted magnetic III-V semiconductors. Phys Rev Lett 1992; 68: 2664-7.

- [4] Matsukura F, Ohno H, Shen A, Sugawara Y. Transport properties and origin of ferromagnetism in (Ga,Mn)As. *Phys Rev* 1998; B 57: R2037-R40.
- [5] Weidemann R, Gumlich H-E, Kupsch M, Middelmann H-U, Becker U. Partial density of Mn 3d states and exchange-splitting changes in Zn_{1-x}Mn_xY (Y = S, Se, Te). *Phys Rev* 1992; B45: 1172-80.
- [6] Sato K, Katayama-Yoshida H. Material design for transparent ferromagnets with ZnO-based magnetic semiconductors. *Jpn J Appl Phys* 2000; 39: L 555-8.
- [7] Sato K, Katayama-Yoshida H. Stabilization of ferromagnetic states by electron doping in Fe-, Co- or Ni-doped ZnO. *Jpn J Appl Phys* 2001; 40: L334-6.
- [8] Sato K, Katayama-Yoshida H. Materials design of transparent and half-metallic ferromagnets in V- or Cr-doped ZnS, ZnSe and ZnTe without P- or N-type doping treatment. *Jpn J Appl Phys* 2001; 40: L651-3.
- [9] Furdyna JK. Diluted magnetic semiconductors. *J Appl Phys* 1988; 64: R29-R64.
- [10] Perdew JP, Wang Y. Pair distribution function and its coupling-constant average for the spin-polarized electron gas. *Phys Rev* 1992; B 46: 12947-54.
- [11] Savrasov SY. Full-Potential program package "LMTART 6.20", User's manual (2000), Max-Planck Institute fuer Festkoerperforschung, D-70569 Stuttgart, Germany. Department of Physics and Astronomy, Rutgers University, Piscataway, NJ 08854. October 12, 2000.
- [12] Blochl P, Jepsen O, Andersen OK. Improved tetrahedron method for brillouin-zone integrations. *Phys Rev* 1994; B 49: 16223.
- [13] Murnaghan FD. On the theory of the tension of the elastic cylinder. *Proc Nat Acad Sci USA* 1947; 30: 244-7.
- [14] Vegard L. The constitution of mixed crystals and the space occupied by atoms. *Z Phys* 1921; 5: 17-26.
- [15] Madelung O, Ed. Landolt Bornstein: Numerical data and functional relationships in science and technology, New Series, Group III, vol.22. Springer: Berlin; 1987.
- [16] Merad AE, Kanoun MB, Merad G, Cibert J, Aourag H. Full-potential investigation of the electronic and optical properties of stressed CdTe and ZnTe. *Mater Chem Phys* 2005; 92: 333-9.
- [17] Imamura M, Okada A. Magneto-optical properties of ZnMnTe Films Grown on Sapphire Substrates. *IEEE Trans Magn* 2006; 42(10): 3078-80.
- [18] Merad AE, Kanoun MB, Goumri-Said S. Ab initio study of electronic structures and magnetism in ZnMnTe and CdMnTe diluted magnetic semiconductors. *J Magn Mater* 2006; 302: 536-42.
- [19] Djemia P, Roussigné Y, Stashkevich A, et al. Elastic properties of zinc blende MnTe. *Acta Physica Polonica A* 2004; 106: 239-47.
- [20] Dynowska E, Przezdziecka E. The crystallographic structure of thin Mn-rich ZnMnTe layers grown by molecular beam epitaxy. *J Alloys Comp* 2005; 401: 265-71.
- [21] Hellwege K-H, Madelung O, Eds. Landolt-Bornstein: Numerical Data and Functional Relationships in Science and Technology, New Series, Group III, Vol. 22a. Springer-Verlag: New York; 1982.
- [22] Lee BH. Pressure Dependence of the Second-Order Elastic Constants of ZnTe and ZnSe. *J Appl Phys* 1970; 41: 2988-90.
- [23] Okoye CMI. First-principles study of the electronic and optical properties of zincblende zinc selenide. *Physica B* 2003; 337: 1-9.
- [24] Santiago RB, Albuquerque e Castro e J, Oliveira LE. Acceptor-related photoluminescence spectra in GaAs-(Ga,Al)As quantum wells: Electric field and doping profile effects. *Brazilian J Phys* 1994; 24: 180-6.
- [25] Rashkeev SN, Lambrecht WRL. Second-harmonic generation of I-III-VI₂ chalcopyrite semiconductors: Effects of chemical substitutions. *Phys Rev B* 2001; 63: 165212-24.
- [26] Morozzi VL, Janak JF, Williams AR. Calculated electronic properties of metals. Pergamon: New York; 1978.
- [27] Gaj JA, Planel R, Fishman G. Relation of magneto-optical properties of free excitons to spin alignment of Mn²⁺ ions in Cd_{1-x}Mn_xTe. *Solid State Commun* 1979; 29: 861-4.
- [28] Szczytko J, Mac W, Twardowski A, Matsukura F, Ohno H. Antiferromagnetic pd exchange in ferromagnetic Ga_{1-x}Mn_xAs epilayers. *Phys Rev B* 1999; 59: 12935-9.
- [29] Schulthess TC, Butler WH. Electronic structure and magnetic interactions in Mn doped semiconductors. *J Appl Phys* 2001; 89: 7021-4.
- [30] Larson BE, Hass KC, Ehrenreich H, Carlsson AE. Theory of exchange interactions and chemical trends in diluted magnetic semiconductors. *Phys Rev B* 1988; 37: 4137-54.
- [31] Twardowski A, Dietl B, Demianiuk M. The study of the s-d exchange interaction in Zn_{1-x}Mn_xSe mixed crystals. *Solid State Commun* 1983; 48: 845-8.
- [32] Ferrand D, Cibert J, Bourgognon C, et al. Equilibrium partial pressures and crystal growth of Cd_{1-x}Zn_xTe / Sang, in p-doped Zn(1-x)MnxTe epilayers. *J Cryst Growth* 2000; 387: 214-15.
- [33] Pollak RA, Ley L, Kowalczyk SP, et al. X-ray photoemission valence-band spectra and theoretical valence-band densities of states for Ge, GaAs, and ZnSe. *Phys Rev Lett* 1972; 29: 1103-5.
- [34] Chelikowsky JR, Cohen ML. Nonlocal pseudopotential calculations for the electronic structure of eleven diamond and zinc-blende semiconductors. *Phys Rev B* 1976; 14: 556.
- [35] Cardona M. Optical studies of the band structure in InP. *J Appl Phys* 1961; 32: 2151.
- [36] Saitta AM, de Gironcoli S, Baroni S. Effects of disorder on the optical properties of the (Zn,Mg)(S,Se) quaternary alloy. *Appl Phys Lett* 1999; 75: 2746.
- [37] Karazhanov SZh, Ravindran P, Kjekshus A, Fjellvåg H, Svensson BG. Electronic structure and optical properties of ZnX (X = O, S, Se, Te): A density functional study. *Phys Rev B* 2007; 75: 155104-18.
- [38] Martienssen W. Landolt-Börstein "Numerical data and functional relationships in science and technology."V17 (Semiconductors), Springer-Verlag: Berlin; 1982.
- [39] Veera Brahmam K, Raja Reddy D, Reddy BK. Crystal growth and reflectivity studies of Zn_{1-x}Mn_xTe crystals. *Bull Mater Sci* 2005; 28(5): 411-14.
- [40] Jolanta S. Electroreflectance and wavelength-modulated reflectivity measurements of Zn_{1-x}Mn_xTe mixed crystals. *J Appl Phys* 1988; 64: 6815-18.
- [41] Bucker R, Gumlich H-E, Krause M. The influence of the temperature and the composition on the reflectivity of Cd_{1-x}Mn_xTe within the spectral range of 1.5 eV ≤ E ≤ 4 eV. *J Phys C: Solid State Phys* 1985; 18: 661-7.
- [42] Olego DJ, Faurie JP, Sivananthan S, Raccach PM. Opto-electronic properties of Cd_{1-x}Zn_xTe films grown by molecular beam epitaxy on GaAs substrates. *Appl Phys Lett* 1985; 47: 1172.
- [43] Janik E, Dynowska E, Bak-Misiuk J, et al. Structural properties of cubic MnTe layers grown by MBE. *Thin Solid Films* 1995; 267: 74.
- [44] Gunshor RL, Nurmikko AV, Kodziejski LA, Kobayashi M, Otsuka N. Wide-gap II-VI heterostructures. *Crystal Growth* 1990; 101: 14-22.
- [45] Fleszar A, Potthoff M, Hanke W. Electronic structure of zinc-blende MnTe within the GW approximation. *Phys Status Solidi C* 2008; 4(9): 3270-9.

Received: September 28, 2008

Revised: November 10, 2008

Accepted: November 11, 2008

© Benkhetou and Bensaïd; licensee *Bentham Open*.This is an open access article licensed under the terms of the Creative Commons Attribution Non-Commercial License (<http://creativecommons.org/licenses/by-nc/3.0/>) which permits unrestricted, non-commercial use, distribution and reproduction in any medium, provided the work is properly cited.